

archives
of thermodynamics

Vol. 41(2020), No. 2, 201–221

DOI: 10.24425/ather.2020.133629

Analysis of non-equidistant baffle spacing in a small shell and tube heat exchanger

ABDULLAH AZIZ^{*a}
SHAFIQUE REHMAN^b

^a Institute of Business and Management, Korangi Creek, Karachi, Pakistan

^b National University of Sciences and Technology. NUST Campus, H-12, Islamabad, Pakistan

Abstract Most of the formulations regarding the characteristics of a shell and tube heat exchanger have a common assumption; namely that the baffle plates are equidistant. This assumption fails to cater the real world scenario for defective baffles as the alteration in a shell and tube heat exchanger invalidates the equidistant baffle spacing of the plates. In this regard, a small six baffles heat exchanger was modeled in the computational fluid dynamics software package and studied by removing each baffle plate one at a time. Effect of removing each baffle plate on the temperature, pressure, heat transfer coefficient, and total heat transfer rate was recorded. It was observed that variation in the pressure drop for the same number of baffle plates varies along the axial order of the plates. The change in pressure drop due to the removal of the baffle plate near the inlet and the outlet was lowest and reaches a maximum in the axial center. It was also found that the plates below the radial center contribute higher towards the overall heat transfer as compared to those above.

Keywords: Thermal distribution; Baffle spacing; Heat exchanger; Turbulence modeling; CFD study

Nomenclature

D_e – equivalent diameter, m

*Corresponding Author. Email: abdullah.aziz@iobm.edu.pk

- D_s – inside diameter of the shell, m
 F – sum of Reynold forces
 f – Fanning friction factor
 G_s – mass velocity on the shell side, kg/s m²
 g – gravitational acceleration, m/s²
 i, j – indices (= 1, 2, 3)
 L_b – distance between two adjacent baffle plates, m
 N_B – number of baffle plates
 p – pressure, Pa
 \mathbf{u} – velocity vector
 u_i – velocity components (along the $x_1=x$, $x_2=y$, and $x_3=z$ axes), m/s
 v – absolute velocity along y -axis, m/s²
 x_j, y – Cartesian coordinates, m

Greek symbols

- β – orientation angle of baffle plate, degrees
 μ – viscosity of fluid in tubes, kg/ms
 μ_s – viscosity of fluid in shell, kg/ms
 ρ – density of the shell-side fluid, kg/m³

Abbreviations

- STHE – shell and tube heat exchangers
 S-A – Spalart and Allmaras

1 Introduction

Heat exchangers are one of the widely used equipment in process industries. They are used to transfer heat between multiple process streams for the purpose of cooling, heating, condensation, boiling, and evaporation. They are categorized according to their mode of contact, flow direction, the number of fluid passes and according to the Tubular Exchanger Manufacturers Association (TEMA) Standards [1]. Efficiency and performance of a heat exchanger are measured in terms of the amount of heat transferred between fluids of the shell and the tubes, and the pressure drop across both shell's and tube's, inlets and outlets [2].

Shell and tube heat exchangers (STHE) consist of baffle plates which, with the passage of time, get corroded. Instead of repairing the baffle, the feasibility of a handicapped heat exchanger is under debate. A handicapped heat exchanger may be defined as a heat exchanger where a single component is removed or bypassed while the remaining geometry remains intact. This practice is common in cases of tube failures [3].

Theoretically, a heat exchanger is designed by a series of formulations and well-defined methods which involve parameter settings such as dimen-

sions, geometry, the positioning of components, physical and thermal properties of the fluid and the solid material used for fabrication. Formulation regarding design parameters for both Kern [4] and Bell-Delaware [5] methods are for equidistant baffle plates. The oldest experimentation carried out on STHE back in 1954 [6] proposed a formula for calculating pressure drop due to the presence of baffle plates in the shell of the heat exchanger [7]

$$\Delta p = \frac{2fG_s^2 D_s (N_B + 1)}{\rho D_e \left(\frac{\mu}{\mu_s}\right)^{0.14}}. \quad (1)$$

During the formulation of this expression, baffle plates were equispaced such that

$$L_b = \frac{L_{shell}}{N_B + 1}. \quad (2)$$

It is concluded that pressure drop is a function of the number of baffle plates as $\Delta p = f(N_B)$. Equation (2) becomes irrelevant in the case of variable baffle spacing as the number of baffle plates (N_B) and length of the shell (L_{shell}) is constant.

The hypothesis being put forward was that by removing a single baffle plate, different values of pressure drop will be obtained depending upon which baffle plate was being removed. In other words, an STHE of n number of baffles will have a single value for pressure drop (Δp_n). For an $n-1$ baffled STHE of the same shell and tube dimensions, the value of pressure drop should be constant (Δp_{n-1}) while our hypothesis claims that there can be n number of values of Δp_{n-1} . For this purpose, instead of fabricating heat exchangers and empirically removing baffle plates, a computational fluid dynamics (CFD) study has been carried out to save resources. An existing study [8] was referred where experimentation was converted to CFD study to compare the accuracy between empirical and numerical results. The heat exchanger used in their research was adapted for our study. Comparing the accuracy of results in a numerical study with experimental results is a well-explored terrain [9–12], . We initially replicated the study in a CFD software package then carried out simulations to validate our hypothesis.

In this article, we have gone through a brief history of various studies on heat exchangers in Section 2. The effects of changes in geometry, different numerical computation methods, and advantages of different types of heat exchangers over one another are also discussed. Section 3 covers the

modelling technique and defines CFD parameters for this study. Results and conclusion are discussed in Section 4 and 5, respectively.

2 Background

Significant work has been done on the shell and tube heat exchangers over the past few decades in various applications. In this section, the effect of the unbaffled heat exchanger, baffle cut, the arrangement of tubes, number of passes, and extended surfaces on the heat transfer of a shell and tube heat exchanger is presented. The advantages and limitations of computational fluid dynamics study are also discussed.

A comprehensive study [13] highlighted the contribution of baffles in the overall heat transfer. Their study was a comparison between baffled and unbaffled vessel under the scenario of forced convection. The study, as expected, concluded that baffled plates helped in agitating the fluid and increasing the heat transfer coefficient values by 41.22%.

Baffle cut (B_c) allows fluid channeling within the shell and ranges from 15% to 45% of the shell diameter. A smaller baffle cut generates more turbulence resulting in a better heat transfer rate at the expense of mass flow rate. The angle between the baffle surface and the radial direction of the shell (β) at which these baffle plates are placed in the shell also affects the heat transfer rate. Positive angle toward the direction of the flow helps in reducing turbulence allowing the STHE to operate at lower values of flow rate [14].

Baffle plates are designed for two purposes; namely to agitate the flow of at the shell side of STHE as well as to maintain the structural rigidity of the exchanger. With variable baffle spacing, the drag force on each baffle will produce a certain torque with respect to its center of gravity and cause vibrations [15]. Structural analysis was set aside in this study. Also, a comparison of two equation turbulence model and a single equation turbulence model was carried out as an extensive analysis.

To assist the whisk of the flow, tubes and sometimes shell is modified with an external coil wrapped around. The performance can be calculated with respect to centrifugal forces acting on the moving fluid [16]. An experimental study was conducted on 32 different STHE concluding that the correlation between the results of two heat exchangers can be used to predict the values of the third one [17]. From an analytical research, expressions were put forward to express heat transfer from the tube banks in a cross

flow STHE [18]. A comparison between inline and staggered arrangement of the tube banks was presented. Results indicated that staggered arrangement gives higher heat transfer rates than the in-line arrangement. STHE can also be modeled using distributed resistance approach where a computation cell can have more than one tubes so that the grid at the shell side of the exchanger can be coarse comparatively [19].

When compared with analytical or empirical solutions, computational fluid dynamics has its limitations. Though it can be used in both rating and iteratively in the sizing of heat exchangers, it helps in reducing the number of prototypes and provides good insights. To run a successful CFD simulation, large computational power is required. Without any simplification, an industrial STHE with 500 tubes and 10 baffles requires up to 150 million elements for computation and resolving the geometry [19]. The model is usually simplified by using basic geometry, truncating long equations, and neglecting omitable parameters. Including all of these simplifications, CFD of the STHE shows good agreement with experimental data [20]. To obtain near accurate results while saving computational power, Spalart and Allmaras proposed a turbulence model for defining the fluid flow [21]. When modelled in a CFD package, the results obtained are similar to those of $k-\varepsilon$ or $k-\omega$ models [8]. Commercial and non-commercial fluid simulation software packages are available to model different types of heat exchangers have very little difference in results for small scaled non-complex industrial application [22].

Usually, two equation $k-\varepsilon$ model is commonly used in industrial designing of STHE. Jae *et al.* [23] studied the use of this model in the industry predicting the new wall treatments and compared it with other turbulence models. Experimental investigation can be carried out by using other methods such as digital particle image velocimetry, where small quantities of non-dissolving reflecting substance are mixed with the fluid under study and imaging is carried out over intense laser beams [24].

In the next section, we have discussed the governing equations behind the simulation and how the heat exchanger was modelled in the computational fluid dynamics software package. Boundary conditions, geometry, and assumptions are also discussed in detail.

3 Modelling

The fluid flow is governed by the continuity equation, the energy equation, and the Navier-Stokes momentum equations [25]. All these equations are being used for this study under a control volume setup. The conservation of mass is described by the continuity equation. For incompressible steady state flow, using index notation ($i, j = 1, 2, 3$), the equation is written as

$$\frac{\partial u_i}{\partial x_i} = 0 . \quad (3)$$

Flow passing through the heat exchanger is fluid at low velocity and considered incompressible. Thus the momentum equation is used as

$$u_j \frac{\partial u_i}{\partial x_j} = -\frac{\partial p}{\partial x_i} + \mu \frac{\partial^2 u_i}{\partial x_j \partial x_j} . \quad (4)$$

For simulation purposes, the momentum equation is combined with the continuity equation to overcome the absence of pressure component in the continuity equation. The combination is a common practice [26] which results in the Poisson equation as

$$\frac{\partial}{\partial x_i} \left(\frac{\partial p}{\partial x_i} \right) = -\frac{\partial}{\partial x_i} \left(\frac{\partial \rho u_i u_j}{\partial x_i} \right) . \quad (5)$$

The primary purpose of the turbulence model is to determine the distribution of Reynolds stresses in order to develop the system of equations governing the mean motion of the flow. Spalart and Allmaras used series of experimentations and hit-and-trial methodologies to obtain a single equation [21], similar to Nee-Kovasznay model [27], where the flow field is defined as

$$\frac{DF}{Dt} = \frac{\partial F}{\partial t} + (\mathbf{u} \cdot \nabla) F = \text{Production} - \text{Destruction} + \text{Diffusion} \quad (6)$$

To construct a full model for turbulent flow, each part of the above equation is expressed in detail. Along the process of defining each variable, certain constants were introduced [21]. The corrections were introduced to remove unnecessary delays in turbulent transitions in (Reynolds-averaged Navier-Stokes) RANS region, which gave rise to various versions of Spalart-Allmaras equation [28].

As mentioned earlier in Section 1, we selected the heat exchanger used in

the study by Ozden and Tari [8], who used Spalart-Allmaras (S-A) and $k-\varepsilon$ turbulence models. We have used specification of their heat exchanger to model ours. This way we get to validate our hypothesis using two models, i.e. a modern one equation model and a classic two-equation model.

3.1 Geometry

The geometry of the heat exchanger selected for this study consists of seven tubes and six baffle plates. It was a single pass heat exchanger with the baffle cut of 36%. The heat exchanger was 0.6 m long and 0.09 m wide with staggered tubes as shown in Fig. 1.



Figure 1: The shell and tube heat exchange mesh indicating inlet, outlet, and baffles.

Data for inlet and outlet area, their positions, relaxation factors, and turbulence velocity ratios were missing in the published reference study [8]. Therefore, our geometry was slightly modified. Square cross-sectional area for inlet and outlet was assumed as 0.0016 m^2 at an offset of 0.022 m from each ends. Relaxation factors and turbulence viscosity ratios were CFD software package defaults and meshing was structured. It can be foreseen that when validating our reference heat exchanger, there might be deviations in results due to these assumptions. This one pass STHE has the parameters shown in Tab. 1.

Table 1: Parameters of reference heat exchangers.

Description	Value	Unit
Shell size	0.09	m
Tube outer diameter	0.02	m
Tube bundle geometry & pitch	0.03	m
Number of tubes	7	–
Heat exchanger length	0.6	m
Shell side inlet temperature	300	K
Baffle cut	36	%
Central baffle spacing	0.086	m
Number of baffles	6	–

The study was a steady state incompressible flow with shell inlet temperature at 300 K. Operating pressure was set at 101 325 Pa and gauge pressure at outlet was set to 0 Pa to obtain the relative pressure drop. Inlet velocity profile was kept uniform, where fluid was moving at a flow rate of 1 kg/s and no-slip condition was applied at each surface. It was assumed that the shell was perfectly insulated hence zero heat flux was observed at shell outer walls. To keep our focus on shell side only, the tube were modeled with constant wall temperatures of 450 K.

For this simulation, second-order upwind scheme for momentum, energy, and modified viscosity equations were selected according to reference heat exchanger study [21]. The inclusion of three data points instead of two increases the accuracy of results dramatically [29]. First order scheme produces more dissipation in the flow while the second order scheme ends up in a limited cycle with good computed results and stability. A limiter, i.e. trimming the higher order values may be introduced in higher-order method for the effect of interpolation on discontinuous data [30].

3.2 Validation

Prior to validating, it is necessary to select an optimum grid size and number of cells before simulation of any case study. This prevents unnecessary number of cells while ensuring the accuracy in results. The grid convergence criterion in our study was to be determined in terms of pressure and temperature values. Initially, the heat exchanger was modelled with 0.15

million cells and then again modelled by raising the cell count to 0.3, 0.7, and 1.4 million cells. We obtained promising results similar to those of our reference at 0.7 million cells. It was observed that there was insignificant difference when increasing the cell count from 0.7 to 1.4 million. Similar results were obtained when repeating the grid independence for the $k-\varepsilon$ model. Near-wall treatment was carried out before the first baffle and after the last baffle around the inlet and outlet regions only. The convergence criterion was taken as 10^{-6} for the pressure residual, and 10^{-3} for all of the other residuals.

The temperature and pressure values of the computational model were compared with the results reported in the reference study. Shell side outlet temperature, shell side outlet pressure, overall heat transfer coefficient, and total heat transfer rate were set as a validation criterion. The error between current simulation and reference simulation was calculated *via* relation

$$\text{Error} = \frac{|\text{Simulation} - \text{Reference Simulation}|}{\text{Reference Simulation}} \times 100 . \quad (7)$$

It was foretold that a certain degree of error will be incurred due to different assumptions against missing data. Error obtained after simulation for shell side outlet temperature, absolute pressure, overall heat transfer coefficient and total heat transfer rate (HTR) was 2.35%, 1.04%, 8.45%, and 7.35%, respectively.

4 Results and discussion

The aim was to find the variation in heat transfer and temperature drop for variable baffle spacing for same shell and tube structure. That is, for a single number of N_B there will exist different values of outlet pressure and temperature with respect to geometric alterations. Note that due to the removal of a baffle plate there will be a lessen stir of the shell side fluid thus the tubes will transfer less heat comparatively, therefore, the outlet temperature will be lower in the handicapped heat exchanger. Similarly, the pressure drop will be reduced and the shell side outlet pressure will be increased.

A total of eight cases were studied. Terminology for case names was in order of '6-#' where '#' represents the position of the plate from the inlet. Each number represents a plate removed in order from A to F as 6-1 to 6-6. Case 6-0 means no plates were removed where the case becomes similar to that of Ozden and Tari. For the case study in which all plates were

removed, '#' was replaced by an 'A'. Table 2 shows the terminology used and results obtained for each case using the Spalart-Allmaras model. Baffle plates were named from A to F such that baffle A was adjacent to inlet and F being adjacent to the outlet as shown in Fig. 2. Focus of the study was

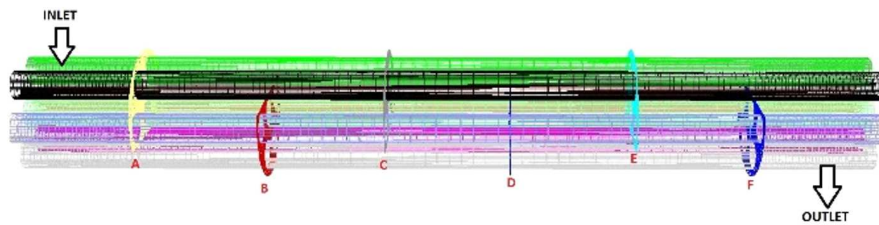


Figure 2: Plate nomenclature and position.

on the effects on temperature and heat transfer values due to alteration in exchanger setup. For this purpose, temperature, velocity, and behavior of the flow were studied in detail. Figure 3 shows three-dimensional velocity streamlines and two-dimensional pressure contours for Case 6-0.

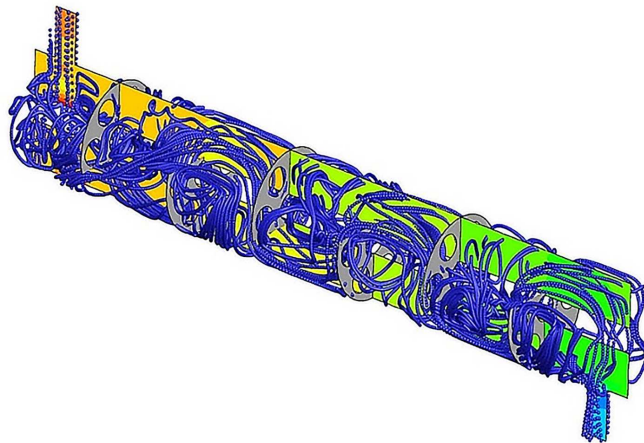


Figure 3: 3D velocity streamlines and 2D pressure contour around Case 6-0.

It was observed that Case 6-1 and Case 6-6 showed similar behavior when compared to Case 6-0. The fluid agitates less and caused around a 0.17%

drop in outlet temperature due to widening of the inlet and the outlet channels due to the absence of the neighboring baffle plate [31,32]. When removing the plate adjacent to either entry or exit region no large vortices were formed. As seen in Case 6-1 and Case 6-6, there was insignificant return-flow of the fluid around the shell wall and the immediate baffle plate.

Table 2: Findings table indicating all cases and results obtained.

Case No.	Plate re-moved	Shell outlet temperature (K)	Shell outlet pressure (Pa)	Heat transfer coefficient (W/m^2K)	Total heat transfer rate (W)
6-0	None	333.96	93751	3345	150272
6-1	A	333.37	94408	3283	147866
6-2	B	331.21	95564	3080	139014
6-3	C	332.06	96102	3156	142403
6-4	D	331.27	95750	3079	139130
6-5	E	331.84	95776	3137	141581
6-6	F	332.90	93867	3162	142783
6-A	All	322.98	98765	2281	105098

Cases 6-2 and 6-4 and case 6-3 and 6-5 were paired together as they showed similar behavior by forming high-temperature regions in absence of the baffle plates. In Case 6-2, as seen in Fig. 4, tubes on top had the least contact time with fluid in the handicapped region. The absence of any uplifting force created large vortices as they hit plate C and agitates to decrease the heat transfer coefficient [33]. The fluid recirculation shown by the thick lines was only occurring due to turbulence.

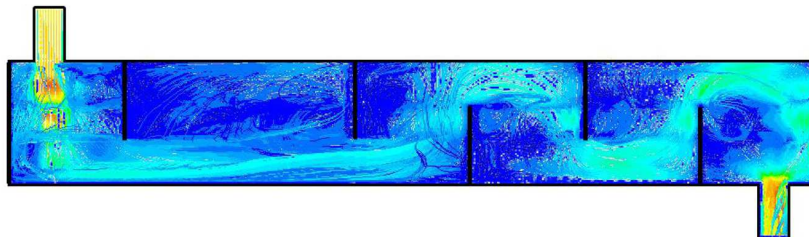


Figure 4: Case 6-2, where plate B (2nd plate from the inlet) was removed.

A similar argument can be put forth in Case 6-4 with an exception that for Case 6-4, the flow remains in contact for a longer period of time before it experiences vortices in the downstream.

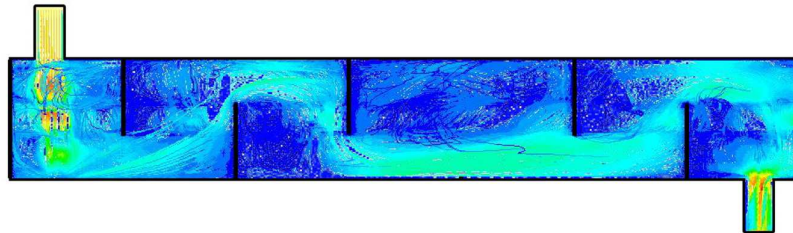


Figure 5: Case 6-4, where plate D (4th plate from the inlet) was removed.

Due to the removal of plate C in Case 6-3, the flow tends to move forward at a higher velocity without any obstruction. The gravitational force pulls the fluid down midway, creating recirculation of the flow (see Fig. 6). The vortex formed in the handicapped region had lower velocity values which resulted in a longer contact time with the tubes resulting in higher outlet temperature. When fluid hits the floor of the shell, it continued to flow with a maximum contact with the lower tubes.

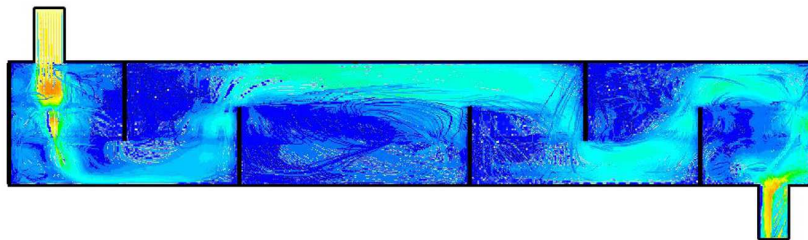


Figure 6: Case 6-3, where plate C (3rd plate from the inlet) was removed.

Case 6-5 was slightly different from Case 6-3. A pull was experiencing by the fluid as it was closer to the shell's outlet. Hence the non-traditional raise in velocity and lesser fluid contact with the tube was observed, which resulted in lower temperature values at the outlet as comparatively. When all baffle plates were removed, Case 6-A acted in an expected manner as a flow in a large pipe with hindrances (tubes) in-between. The loss of temperature rise was up to 3.28% and pressure drop was reduced by 5.34%.

Nodal values of temperature and velocity parameters were considered

on an imaginary line as $y - 11 = 0$ as shown by offset line in Fig. 7.

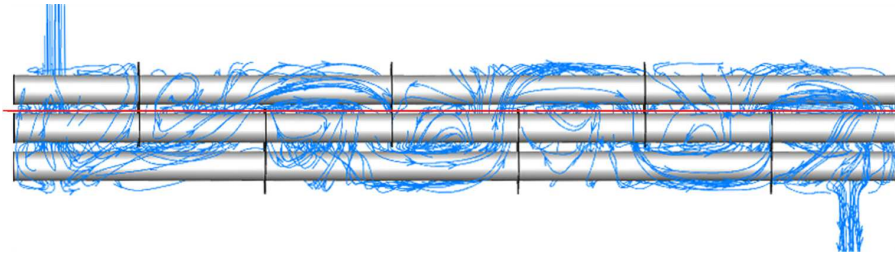


Figure 7: Imaginary line $y - 11 = 0$ indicated with the orange line as viewed from x -plane.

This imaginary line was exactly 0.001 m above the central tube of the heat exchanger. Static temperature and absolute velocity were calculated as $v = \sqrt{u_1^2 + u_2^2 + u_3^2}$. The change in static temperature along the line $y - 11 = 0$ for each case can be seen in Fig. 8, where origin was taken at the center of a circular shell wall near inlet.

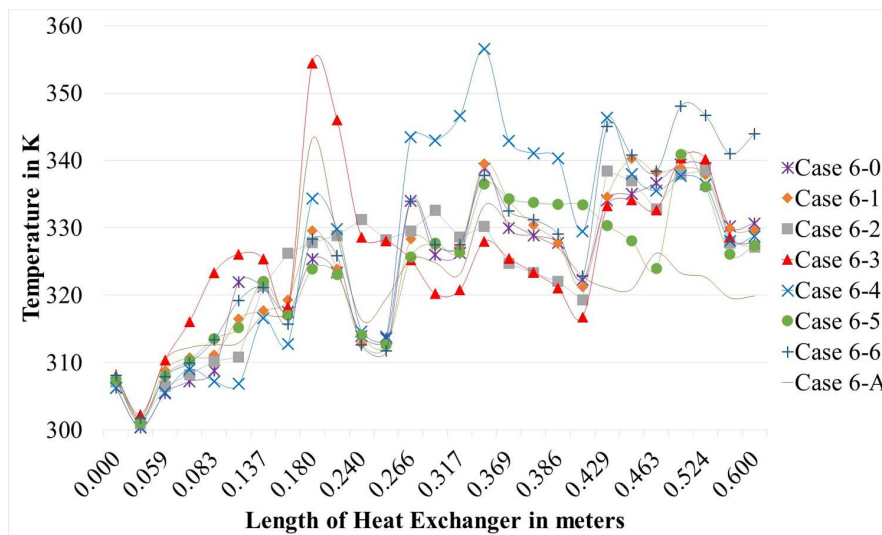


Figure 8: Static temperature along the length starting from the shell inlet face.

The abscissa represents the distance traveled by the fluid from the shell face at inlet to the shell face at outlet while the ordinate represents the temperature in kelvins. The curve dropped from 0.024 to 0.035 m were due to positions of the inlet channel. A sinusoidal behavior was observed

in each case. Peaks formation were just before the baffle plates. The baffle cut of 36% means baffle trims at 0.0576 m from either floor or roof or at line $y - 12.6 = 0$. The 0.0016 m region adjacent to each baffle where fluid was denser which resulted in high localized temperature values. In Fig. 8, the peaks in temperature values due to baffle plates emerged around 0.083 m (baffle A at 0.086 m), 0.180 m (baffle B at 0.172 m), 0.266 m (baffle C at 0.258 m), 0.343 m (baffle D at 0.344 m), 0.420 m (baffle E at 0.430 m) and 0.506 m (baffle F at 0.516 m) away from shell inlet wall.

For Case 6-6, the temperature rises in the last section of the shell. When the fluid passes the fifth baffle plate E, it experienced the remaining region as a discharge channel for the shell outlet. Change in the velocity magnitude of each case was observed (Fig. 9) over the same imaginary line $y - 11 = 0$. The fluid falls directly onto the tube in the middle of the cluster as shown in Fig. 10, and the peaks at 0.040 m were due to splash return of the fluid after hitting this tube. It was observed that fluid velocity was calculated twice, when fluid passes through the line when entering the shell and when fluid rebounds from middle tube and passing through the line again. Higher of the two values are shown in Fig. 9.

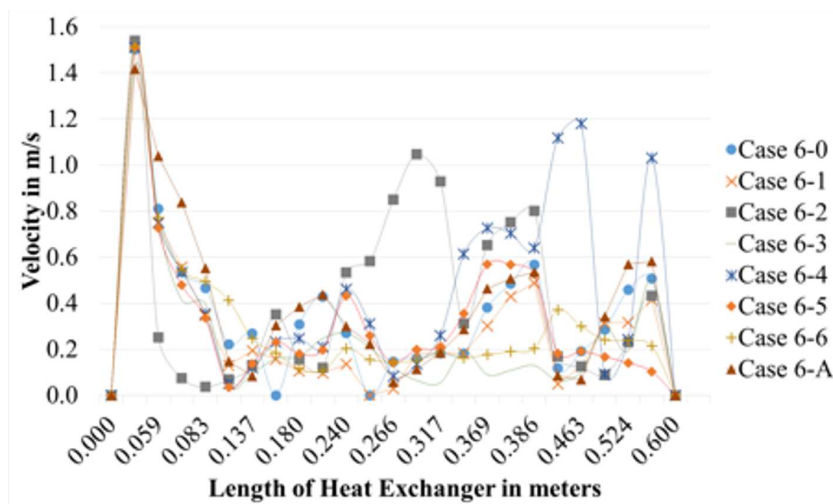


Figure 9: Velocity magnitude along the length starting from the shell inlet face.

Last peak, maximum at 0.583 m was around the shell outlet. All cases show peaks around the same region. Interestingly, Case 6-6 shows its last peak at somewhere around 0.525 m which was where the last baffle plate

was present. As stated earlier, the fluid, in this case, finds the whole region as an outlet channel. Note that all the curves experience similar dome formation notably in Case 6-2 and Case 6-4 was due to vortex formation at the absence of the baffle plate. Case 6-4 shows unique magnitudes of velocity at the exit region as it was experiencing a return flow due to baffle E as shown in Fig. 6.

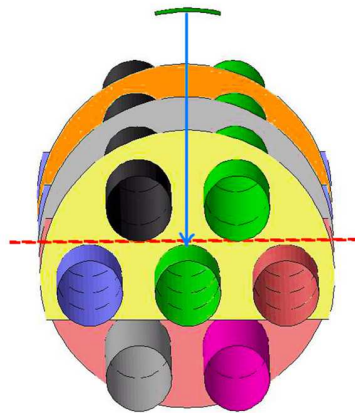


Figure 10: Imaginary line $y - 11 = 0$ as viewed from y -plane.

Same methodology was used for plotting velocity magnitude along seven similar imaginary lines with the increment or decrement of 11 such as $y - 22 = 0$, $y - 33 = 0$, $y - 44 = 0$, $y + 11 = 0$, $y + 22 = 0$, $y + 33 = 0$ and $y + 44 = 0$. As suspected, all positive y -axis showed a similar trend but with variation in magnitude (see Fig. 11). The vortex formed in each baffle section was stronger in the middle of the baffle plate, i.e. for line $y - 22$ and $y - 33$, and weaker at the edges or corners of the section ($y - 11$ and $y - 44$).

Interestingly, when going below the axis (negative axis), the trend found was similar to that of the positive axis (Fig. 12). The domes were formed on the alternating regions and the velocities at the inlet ranged from highest to lowest in normal manner. For positive axis, the exit region showed high velocities just before the exit region.

All cases were executed again using the $k-\varepsilon$ realizable model with standard wall functions. Both cases show similar results. The $k-\varepsilon$ model, as suspected, produces more accurate results near to Ozden and Tari's exper-

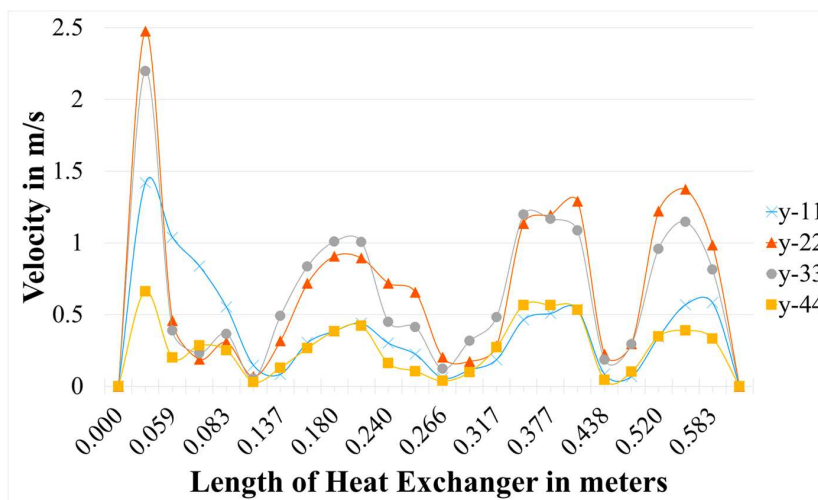


Figure 11: Velocity magnitude along positive y -axis.

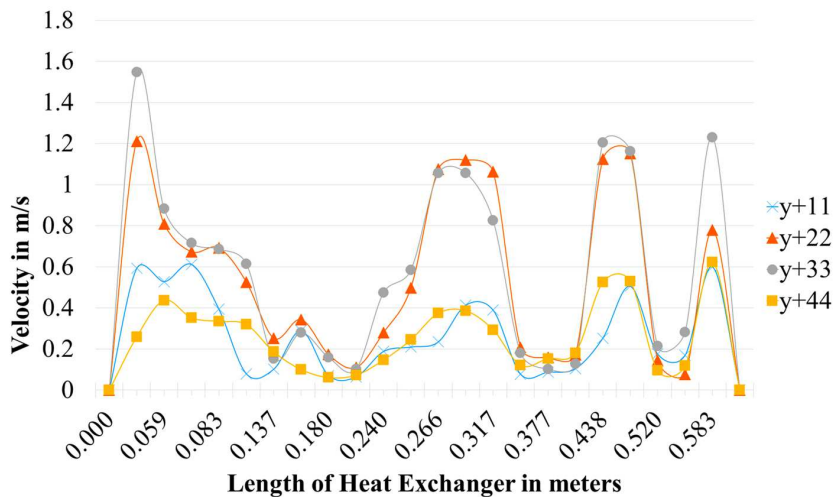


Figure 12: Velocity magnitude along negative y -axis.

imental results [8]. Following chart (Fig. 13) indicates the change in values of shell side outlet temperature in each case as we move from baffle A to baffle F.

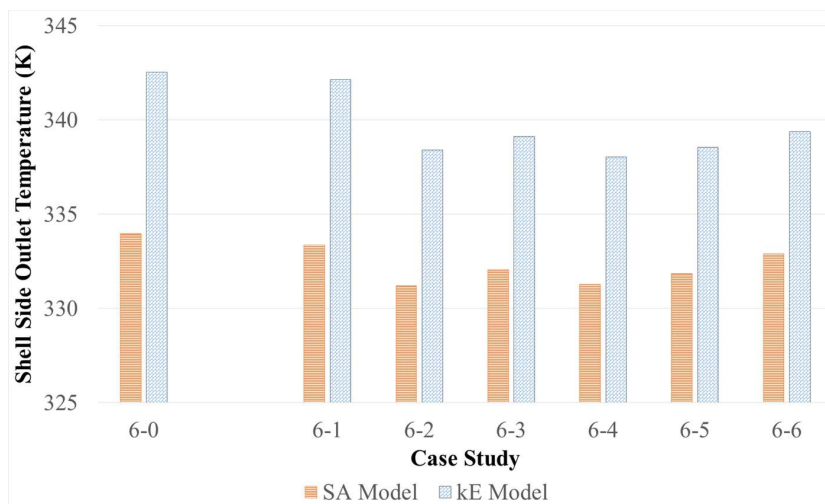


Figure 13: Comparison of shell side outlet temperature for Spalart-Allmaras model and $k-\varepsilon$ model in each case study.

As the overall heat transfer coefficient and the total heat transfer is dependent upon temperature, both parameters showed similar charts as shown in Fig. 14 and 15, respectively. The peak value in Case 6-3, as mentioned earlier, was due to large recirculation flows in handicapped regions causing fluid to be locally heated for a longer period of time.

The $k-\varepsilon$ model also showed a similar trend in results. The peaks formed were sinusoidal as those in Spalart-Allmaras (S-A) model. This proved that the change of turbulence model contributes to the accuracy of results. When removing a plate, the baffle spacing for that region was doubled, i.e. from 0.086 m to 0.172 m. Fluid flowing in the lower half of the exchanger made the exit channel thrice of actual baffle spacing and bypassing the baffle above. This resulted in lower outlet temperatures. In Fig. 16, the shell side absolute pressure graph indicates that pressure drop was higher if the baffle plates were removed immediately after inlet and outlet. This was because the fluid finds the whole region as a discharge channel.

Removal of first and last plate results in a change in pressure of 657 Pa and 116 Pa. For removing a single baffle plate, we were able to calculate 6 different values of pressure drops provided all the remaining parameters were not changed.

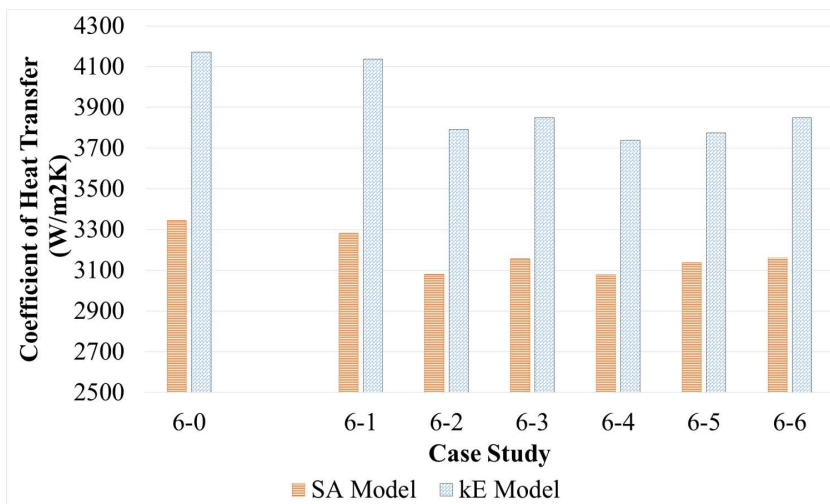


Figure 14: Comparison of coefficient of heat transfer for Spalart-Allmaras model and $k-\epsilon$ model in each case study.

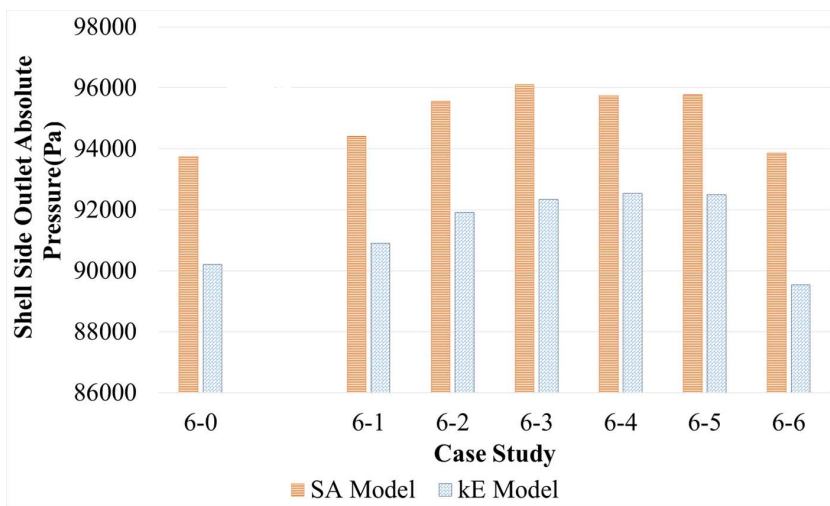


Figure 15: Comparison of shell side outlet pressure for Spalart-Allmaras model and $k-\epsilon$ model in each case study.

5 Conclusion

When considering the pressure drop across the shell side of a shell-and-tube heat exchanger, the structure is always assumed to have an equidistant

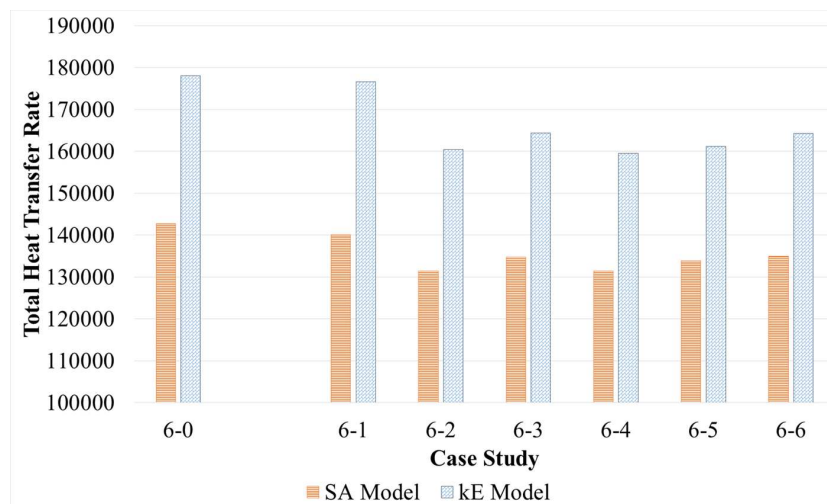


Figure 16: Comparison of total heat transfer rate for Spalart-Allmaras model and $k-\varepsilon$ model in each case study.

baffle spacing. A hypothesis was put forward that when removing a baffle plate, instead of obtaining single value of pressure drop, different values may be observed depending on which baffle is removed. To test our theory, a heat exchanger was modelled from an existing computational fluid dynamics study. The theory was validated as removing a single baffle plate produced different values of pressure drops ranging from 116 Pa to 2351 Pa and loss in temperature gain at shell side ranged from 0.59 K to 2.75 K. The accuracy of results between Spalart-Allmaras model and $k-\varepsilon$ model was appealing and both displayed similar trends in heat transfer coefficients and overall heat transfer rate. The variance in results proved our hypothesis to be true. Further studies can be carried out regarding multiple unequal distances between different pairs of baffle plates in different orders and different combinations. Other turbulence models can be used to further verify the study. This study was limited to fixed number of baffle plates. A comprehensive study can be conducted, either analytical or experimental, to rewrite the Bergelin formula with the provision of variable baffle distance for the same number of baffles.

References

- [1] SHAH R.K., SEKULIC D.P.: *Fundamentals of Heat Exchanger Design*. Wiley, New Jersey 2003.
- [2] BROGAN R.J.: *Shell and tube heat exchangers*. <https://www.wcrhx.com/shell-and-tube-heat-exchangers> (accessed 5 Dec. 2018).
- [3] MENG J.-A., LIANG X.-G., CHEN Z.-J., LI Z.-X.: *Experimental study on convective heat transfer in alternating elliptical axis tubes*. *Exp. Therm. Fluid Sci.* **29**(2005), 4, 457–465.
- [4] KERN D.Q.: *Process Heat Transfer*. McGraw-Hill, 1950.
- [5] SERTH R.W., LESTINA T.: *Process Heat Transfer, Principles and Applications*. Elsevier, San Diego 2007.
- [6] BERGELIN O.P., BROWN G.A., COLBURN A.P.: *Heat transfer and fluid friction during flow across banks of tubes. Part V: A study of a Cylindrical Baffled Exchanger without Internal Leakage*. *Trans. Am. Soc. Eng.* **1**(1954), 76, 841–850.
- [7] PETERS M., TIMMERHAUS K., WEST R.: *Plant Design and Economics for Chemical Engineers*. McGraw-Hill, New York 2002.
- [8] OZDEN E., TARI I.: *Shell side CFD analysis of a small shell and tube heat exchanger*. *Energ. Convers. Manag.* **51**(2010), 5, 1004–1014.
- [9] MA B., RUWET V., CORIERI P., THEUNISSEN R., RIETHMULLER M., DARQUENNE C.: *CFD simulation and experimental validation of fluid flow and particle transport in a model of alveolated airways*. *J. Aerosol Sci.* **40**(2009), 5, 403–414.
- [10] OBERKAMPF W.L., BARONE M.F.: *Measures of agreement between computation and experiment: Validation metrics*. *J. Comput. Phys.* **217**(2006), 1, 5–36.
- [11] VARGA S., OLIVEIRA A.C., MA X., OMER S.A., RIFFAT W.Z.S.B.: *Comparison of CFD and experimental performance results of a variable area ratio steam ejector*. *Int. J. Low-Carbon Technol.* **6**(2010), 2, 119–124.
- [12] ABDULKADIR M., HERNANDEZ-PEREZ V., LO S., LOWNDES I.S., AZZOPARDI B.J.: *Comparison of experimental and computational fluid dynamics (CFD) studies of slug flow in a vertical 90 bend*. *J. Comput. Multiph. Flow.* **5**(2013), 4, 265–281.
- [13] ALDOORI H., BERTRAND J., CHERGUI N., DEBAB A.: *An investigation of heat transfer in a mechanically agitated vessel*. *J. Appl. Fluid Mech.* **4**(2011), 2, 43–50.
- [14] MUKHERJEE R.: *Effective design shell-and-tube heat exchanger*. *Chem. Eng. Prog.* **94**(1998), 2, 21–37.
- [15] *Heat Exchangers Manual*. Flo Fab Inc., Lake Worth 2009.
- [16] ANDRZEJCZYK R., MUSZYŃSKI T.: *Performance analyses of helical coil heat exchangers. The effect of external coil surface modification on heat exchanger effectiveness*. *Arch. Thermodyn.* **37**(2016), 4, 137–159.
- [17] AICHER T., KIM W.K.: *Experimental investigation of heat Transfer in shell and tube heat exchangers without baffles*. *Korean J. Chem. Eng.* **2**(1997), 14, 93–100.
- [18] KHAN W.A., CULHAM J., YOVANOVICH M.: *Convection heat transfer from tube banks in crossflow: Analytical approach*. *Int. J. Heat Mass Transf.* **49**(2006), 4831–4838.

- [19] PRITHIVIRAJ M., ANDREWSA M.J.: *Three Dimensional numerical simulation of shell and tube heat exchangers. Part I: Foundation and fluid mechanics*. Numer. Heat Transfer A: Appl. **33**(1998), 8, 799–816.
- [20] REHMAN U.U.: *Heat Transfer Optimization*. Chalmers University of Technology, Goteborg 2011.
- [21] SPALART P., ALLMARAS S.: *A one-equation turbulence model for aerodynamic flows*. Rech. Aerospat. **1**(1994), 5–21.
- [22] BHUTTA M.M.A., HAYAT N., BASHIR M.H., KHAN A.R., AHMAD K.N., KHAN S.: *CFD applications in various heat exchangers design: A review*. Appl. Therm. Eng. **32**(2011), 1–12.
- [23] KIM J.Y., GHAJAR A., TANG C., FOUTCH G.L.: *Comparison of near-wall treatment methods for high Reynolds number backward-facing step flow*. Int. J. Comput. Fluid Dyn. **19**(2005), 7, 493–500.
- [24] KARAS M., ZAJAC D., ULBRICH R.: *Experimental investigation of heat transfer performance coefficient in tube bundle of shell and tube heat exchanger in two-phase flow*. Arch. Thermodyn. **35**(2014), 1, 89–98.
- [25] ANDERSON J.D.: *Computational Fluid Dynamics for Engineers*. Cambridge University Press, New York 2010.
- [26] FLETCHER C.: *Computational Techniques for Fluid Dynamics*, Vol. I. Springer, Berlin 1991.
- [27] NEE V.W., KAVASZNY L.S.G.: *Simple phenomenological theory of turbulent shear flow*. Phys. Fluids **12**(1969), 473–484.
- [28] RUMSEY C.: *Spalart-Allmaras Model*. Langley Research Center NASA, 2018. <https://turbmodels.larc.nasa.gov/spalart.html> (accessed 5 Dec. 2018).
- [29] HOFFMAN K.A., CHIANG S.T.: *Computational Fluid Dynamics*, Vol. I. Michigan Engineering Education System, 2000.
- [30] MURMAN E.M., ABARBANEL S.S.: *Progress and Supercomputing in CFD*. Springer, Boston 1984.
- [31] ZHANG Z., LI Y.: *CFD simulation on inlet configuration of plate-fin heat exchangers*. Cryogenics **43**(2003), 12, 673–678.
- [32] BARTOSZEWICZ J., BOGUSLAWSKI L.: *Numerical analysis of the steam flow field in shell and tube heat exchanger*. Arch. Thermodyn. **37**(2016), 2, 107–120.
- [33] CHILTON T.H., DREW T.B., JEBENS R.H.: *Heat transfer coefficients in agitated vessels*. Ind. Eng. Chem. **36**(1944), 6, 510–516.
- [34] PAL E., KUMAR I., JOSHI J.B., MAHESHWARI N.K.: *CFD simulations of shell-side flow in a shell-and-tube type heat exchanger with and without baffles*. Chem. Eng. Sci. **143**(2016), 314–340.
- [35] SKAGESTAD B., MILDENSTEIN P.: *District Heating and Cooling Connection Handbook*. International Energy Agency, Paris 1999.
- [36] DONAA M.H.K., JALALIRABD M.R.: *Software evaluation via a study of deviations in results of manual and computer-based step-wise method calculations for shell and tube heat exchangers*. Int. J. Appl. Sci. Eng. **2**(2014), 12, 114–126.